

# A Novel estimation and Correction of Channel errors in LTE SYSTEMS

G. Harsha Vardhan  
M.Tech student  
Eluru College of Engg& Tchnology  
Eluru,AP,INDIA  
gurajada.vardhan@gmail.com

R. Mohana Ranga Rao  
Asst.Professor of ECE  
Eluru College of Engg& Tchnology  
Eluru,AP,INDIA  
mohanarangarao@gmail.com

**Abstract:-** The increase in the number of RF devices and the requirement for large data rates places major role in increasing demand on bandwidth. This necessitates the need for RF communication systems with increased throughput and capacity. MIMO-OFDM is one way to meet this basic requirement. OFDM is used in many (WCD) wireless communication devices and offers high spectral efficiency and resilience to multipath channel effects. Though OFDM is very sensitive to synchronization errors, it makes the task of channel equalization simple. MIMO utilize the multiple antennas to increase throughput without increasing transmitter power or bandwidth.

This project presents an introduction to the (MPC) multipath fading channel and describes an appropriate channel model. Many modulation schemes are presented (i.e. BPSK, QPSK, QAM) that are often used in Conjunction with OFDM. Mathematical modeling and analysis of OFDM are given along with a discrete implementation common to modern RF communication systems. Synchronization errors are modeled mathematically and simulated, as well as techniques to estimate and correct those errors at the receiver accurately.

**Key words:** throughput, MIMO-OFDM, synchronization errors, multipath fading.

\*\*\*\*\*

## 1. INTRODUCTION:

Future wireless communication systems demand high data rates operating in wide propagation scenarios that comply with International Mobile Telecommunications-Advanced (IMT-advanced) requirements. The key features of OFDM systems Comprise of robustness against the presence of severe multipath channel conditions, higher spectral efficiency and minimize the effects of Inter-Symbol Interference (ISI) [4]. For preserving the orthogonally among carriers, cyclic prefix or guard intervals are inserted among the subcarriers. The length of the cyclic prefix should be longer than the delay spread of the channel to avoid ISI.

When the transmitter does not possess Channel State Information (CSI) this combinational system can achieve very high spectral efficiency. MIMO-OFDM systems are very sensitive to synchronization errors. The overall performance of the system gets deteriorated in the presence of timing and frequency offsets. The main objective of symbol timing synchronization is to detect the start of the received OFDM symbol. For this purpose either data-aided or non-data-aided timing synchronization can be used. Data-aided refers to synchronization using training sequences. Non-data-aided timing synchronization algorithms perform synchronization by estimating the timing and frequency characteristics of received signal. Most of the timing synchronization algorithms are based on preamble approach [1],[2] because of low computational complexity, fast synchronization speed and high estimation accuracy. This paper is organized as follows. Section 2 briefly introduces the OFDM system model. Section 3 describes the proposed method and the algorithm. Synchronization errors are modeled mathematically and simulated, as well as techniques to estimate and correct those errors at the

receiver accurately using MATLAB simulation is given in Section 4. Finally; the whole paper is concluded in Section 5.

## 2. OFDM System

Figure 1 shows OFDM system block diagram. The principle of OFDM posits that for high speed communications, frequency selective channel is evenly divided into N frequency flat subchannels. These dissevered parallel subcarriers are spaced orthogonal with their inter-carrier spacing tantamount to inverse of symbol duration and spectral peak of individual subcarrier must co-occur with the zero-crossings of other subcarriers [4].

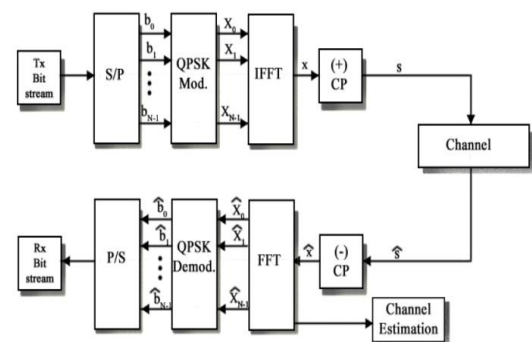


Fig. 1 OFDM system

## 3. PROPOSED WORK

The most challenging aspect of designing a communication system is the estimation and correction of synchronization errors that occur during transmission. 2 shows the block diagram of the synchronization process of a typical receiver. Simulations of the error estimations are

presented using the IEEE802.11 standard for the OFDM frame structure

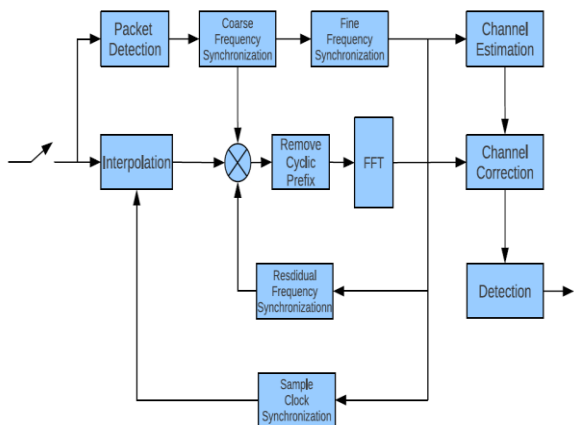


Figure 2 Synchronization blocks in OFDM receiver.

### 3.1 SYNCHRONIZATION ERRORS

OFDM systems are very sensitive to frequency offsets between transmitter and receiver when modulating to pass band and back to baseband. Both ISI and inter channel interference (ICI) need to be mitigated as much as possible in order for the system to accurately receive data.

ICI is affected by the orthogonality of the subcarriers, which can be caused by Doppler shift or the offset in carrier frequency between the transmitter and receiver. Not only must frequency offsets be dealt with but also the sample clock and the frame or FFT window timing. Offsets in timing can cause ISI as well as ICI.

#### 3.1.1 Frequency Offset

Let  $\Delta f_c$  [Hz] be the carrier frequency offset and the normalized carrier frequency offset,  $\varepsilon$ , be

$$\varepsilon = \frac{\Delta f_c}{\Delta f} \quad (1)$$

Where  $\Delta f$  is the sub-carrier bandwidth (sub-carrier spacing). There is not only the possibility of carrier frequency offset between transmitter and receiver, but also a phase difference  $\theta_0$ . As before, let  $x[k]$  be the transmitted sample and  $h[k]$  the  $K^{th}$  tap of the multipath channel impulse response with  $N_c$  taps. Then, the received  $n$ th estimated symbol is

$$\hat{X}[n] = \frac{1}{N} \sum_{k=0}^{N-1} \left( \sum_{l=0}^{N_c-1} h[l] x[k-l] \right) e^{-j2\pi \frac{nk}{N}} e^{j2\pi \frac{k\varepsilon}{N}} e^{j\theta_0} \quad (2)$$

Where  $e^{-j2\pi \frac{nk}{N}}$  performs the demodulation via the FFT,  $e^{j2\pi \frac{k\varepsilon}{N}}$  is the normalized carrier frequency, and  $e^{j\theta_0}$  is the common phase rotation. Evaluating  $\hat{X}[n]$  further we have

$$\hat{X}[n] = \frac{1}{N} \sum_{k=0}^{N-1} \sum_{l=0}^{N_c-1} h[l] \sum_{m=0}^{N-1} X[m] e^{-j2\pi \frac{km}{N}} e^{-j2\pi \frac{nk}{N}} e^{j2\pi \frac{k\varepsilon}{N}} e^{j\theta_0}$$

$$= X[n] H[n] e^{j\theta_0} \frac{e^{j\pi \left(1 + \frac{1}{N}\right) \varepsilon} \sin(\pi \varepsilon)}{\sin\left(\pi \frac{\varepsilon}{N}\right)} + \sum_{m=0, m \neq n}^{N-1} X[m] H[m] e^{j\theta_0} \frac{e^{j\pi \left(m-n + \varepsilon\right) \left(1 + \frac{1}{N}\right)} \sin(\pi (m-n + \varepsilon))}{\sin\left(\pi \frac{(m-n + \varepsilon)}{N}\right)} e^{j\theta_0} \quad (3)$$

The first summand in equation 3 is the desired demodulated symbol on the  $n$ th sub-carrier with attenuation

$$\left( \frac{\sin(\pi \varepsilon)}{\sin\left(\pi \frac{\varepsilon}{N}\right)} \right) \text{ and phase rotations } \frac{e^{j\pi \varepsilon \left(1 + \frac{1}{N}\right)}}{N} \text{ and } e^{j\theta_0}.$$

The second addend is the contribution of the remaining  $N-1$  sub-carriers with attenuation

$$\left( \frac{\sin(\pi (m-n + \varepsilon))}{\sin\left(\pi \frac{(m-n + \varepsilon)}{N}\right)} \right) \text{ and phase rotation } \frac{e^{j\pi (m-n + \varepsilon) \left(1 + \frac{1}{N}\right)}}{N} \text{ and } e^{j\theta_0}.$$

This second summand results in ICI. The coefficients for the second summand are called the ICI coefficients and are described for the  $k$ th sub-carrier index as

$$ICI_N(k) = \frac{e^{j\pi (k + \varepsilon) \left(1 + \frac{1}{N}\right)}}{N} \left( \frac{\sin(\pi (k + \varepsilon))}{\sin\left(\pi \frac{(k + \varepsilon)}{N}\right)} \right) \quad (4)$$

with  $q = 0.5, 0.1, 0.05, 0.025$ .

$$\sum_{k=1}^{N-1} |ICI_N(k)|^2 \quad (5)$$

Another helpful description is the carrier-to-interference power ratio [5] (CIR), which is analogous to SNR, is defined as

$$CIR = \frac{|ICI_N(0)|^2}{\sum_{k=1}^{N-1} |ICI_N(k)|^2} \quad (6)$$

#### 3.1.2 Sampling Clock Offset

At the receiver the incoming signal is sampled with an analog to digital converter (ADC). The ADC is driven by the receiver clock which, in practice, is not perfectly synchronized with the transmitter clock. where frequency offset was considered. To simplify the derivation, we assume an ideal channel with no other synchronization error

present and no cyclic prefix. Let T and T' be the transmitter and receiver sampling periods respectively and q= T-T' T be the sampling period offset. The continuous time transmitted signal is then

$$S_k(t) = \frac{1}{Nfft} \sum_{l=0}^{Nfft-1} X[l] e^{j2\pi l \frac{t}{NfftT}} \quad (7)$$

and the sampled signal at the output of the ADC with sampling period offset

$$\begin{aligned} \varepsilon &= \frac{T' - T}{T} \text{ is} \\ r[nT'] &= s[nT'] \\ &= \frac{1}{Nfft} \sum_{l=0}^{Nfft} X[l] e^{j2\pi l \frac{nT'}{NfftT}} \\ &= \frac{1}{Nfft} \sum_{l=0}^{Nfft} X[l] e^{j2\pi l \frac{n(1+\varepsilon)}{NfftT}} \end{aligned} \quad (8)$$

The attenuation is dependent on sub-carrier index, sampling offset, and the number of sub-carriers. This would suggest that as the sub-carrier index increases, the attenuation decreases and the phase increases. Upon applying the baseband demodulation, the m<sup>th</sup> sub-carrier is

$$\bar{X}[m] = \sum_{n=0}^{Nfft} S[nT'] e^{-j2\pi \frac{nm}{Nfft}} \quad (9)$$

$$= \frac{1}{Nfft} X[m] e^{j\pi m \varepsilon \left(1 + \frac{1}{Nfft}\right)} \left( \frac{\sin(\pi m \varepsilon)}{\sin\left(\pi m \frac{\varepsilon}{Nfft}\right)} \right) + \frac{1}{Nfft} \sum_{l=0, l \neq m}^{Nfft} X[l] e^{j\pi(l(1+\varepsilon)-m)\left(1 + \frac{1}{Nfft}\right)} \left( \frac{\sin(\pi(l(1+\varepsilon)-m))}{\sin\left(\pi \frac{(l(1+\varepsilon)-m)}{Nfft}\right)} \right) \quad (10)$$

As with frequency offset, we have the desired demodulated sub-carrier X[m] with attenuation factor

$$\left( \frac{\sin(\pi m \varepsilon)}{\sin\left(\pi m \frac{\varepsilon}{Nfft}\right)} \right) \text{ and phase rotation } e^{j\pi m \varepsilon \left(1 + \frac{1}{Nfft}\right)}. \text{By}$$

comparison, recall that the attenuation and phase for frequency offset is solely dependent on the frequency offset. Also present is ICI caused by the interaction of the remaining Nfft-1 sub-carriers

$$ICI_\varepsilon[m] = \frac{1}{Nfft} \sum_{l=0, l \neq m}^{Nfft} X[l] e^{j\pi(l(1+\varepsilon)-m)\left(1 + \frac{1}{Nfft}\right)} \left( \frac{\sin(\pi(l(1+\varepsilon)-m))}{\sin\left(\pi \frac{(l(1+\varepsilon)-m)}{Nfft}\right)} \right) \quad (11)$$

where the ICI caused by the lth index is dependent on the desired sub-carrier index m and the sampling offset. To find the the power of the ICI, we assume that the X[k] are independently identically distributed (IID) so that

$$\begin{cases} E[X_k] = 0 \\ E[X_k X_r^*] = \delta_{k,r} \sigma_x^2 \end{cases} \quad (12)$$

where  $\sigma_x^2$  is the expected value of the power in the data symbols. The power of the ICI for the m<sup>th</sup> demodulated sub-carrier is then

$$E[ICI_\varepsilon(m)ICI_\varepsilon^*(m)] = \frac{1}{Nfft^2} \sum_{k=0, k \neq m}^{Nfft} E[X[k]X^*[k]] \left( \frac{\sin(\pi(k(1+\varepsilon)-m))}{\sin\left(\pi \frac{(k(1+\varepsilon)-m)}{Nfft}\right)} \right)^2 \quad (13)$$

$$= \frac{\sigma_x^2}{Nfft^2} \sum_{k=0, k \neq m}^{Nfft} \left( \frac{\sin(\pi(k(1+\varepsilon)-m))}{\sin\left(\pi \frac{(k(1+\varepsilon)-m)}{Nfft}\right)} \right)^2 \quad (14)$$

The signal to ICI power ratio is given by

$$SIR = \frac{|S_k(t)|}{E[ICI_\varepsilon(m)ICI_\varepsilon^*(m)]} \quad (15)$$

### 3.1.3 Frame Timing Offset

The estimation of the OFDM symbol or frame start position determines the alignment of the FFT window with the non-cyclically extended OFDM symbol. An offset in the FFT window can then include a neighboring OFDM symbol causing ISI, which can affect the orthogonality of the sub-carriers producing ICI. Analysis of the effects of frame timing offset on the constellation and the spectrum will be discussed with and without the use of a cyclic prefix for QPSK. Assuming no other synchronization errors and an ideal channel, the time series samples for the m<sup>th</sup> OFDM symbol are

$$x_m[n] = \sqrt{\frac{1}{Nfft}} \sum_{k=0}^{Nfft-1} X_m[k] e^{j2\pi \frac{kn}{Nfft}} \quad (16)$$

for 0 ≤ n ≤ Nfft-1 and sub-carriers 0 ≤ k ≤ Nfft-1. The received signal with channel impulse response hm[n] and AWGN zm[n] is

$$r[n] = \sum_{k=0}^{Nc-1} x_m[k] h_m[n-k] + z_m[n] \quad (17)$$

for channel impulse length Nc. The demodulated symbol is then

$$\bar{X}_m[l] = \sqrt{1/Nfft} \sum_{n=0}^{Nfft} (r_m[n]) e^{-j2\pi \frac{ln}{Nfft}} \quad (18)$$

$$= \sqrt{1/Nfft} \sum_{n=0}^{Nfft} \left( \sum_{k=0}^{Nc-1} x_m[k] * h_m[n-k] \right) e^{-j2\pi \frac{ln}{Nfft}} \quad (19)$$

$$= X_m[l] H_m[l] + Z_m[l] \quad (20)$$

where  $Zm[1]$  is the FFT of the additive Gaussian noise.

### 3.2 SYNCHRONIZATION ERROR ESTIMATION

Synchronization is separated into two categories, acquisition and tracking. In acquisition we focus on carrier frequency offset estimation, symbol timing and frame start position using the preamble structure outlined in IEEE802.11a [7]. Tracking occurs after the preamble has been sent and relies on information embedded into each OFDM frame to ensure carrier frequency and sample clock are locked during transmission.

#### 3.2.1 Preamble Structure of IEEE802.11a

Because of the sensitivity that OFDM has to frequency and timing offsets, measurements must be taken to estimate and correct these offsets at the receiver. To accomplish this and other signal processing functions, four OFDM symbols are prepended to the OFDM burst transmission to aid in acquisition. After this preamble is processed, each successive frame contains four pilot symbols that are used for tracking frequency and timing.

Both the symbols in the preamble and the pilot symbols are known to the receiver. The first two OFDM frames contain ten short preambles and are used for automatic gain control, diversity selection, timing acquisition, and coarse frequency acquisition. We will focus our attention on the acquisition of timing and frequency. The zero packing has the effect of decreasing the symbol time by four, or  $Nfft/4$ , thus yielding the four copies in the time series. Thus, the short training symbols have  $2.5 \times Nfftsymbols$ . In our application of OFDM, IEEE 802.11a/g, the bandwidth is 20MHz and the sample time is  $1/20MHZ = 0.05\mu s$ . If we set  $Nfft= 64$ , as in IEEE802.11a, there are 16 samples in the short training symbol and so the symbol time is  $16 \times 0.05\mu s = 0.8\mu s$ . There are ten short training symbols which gives a total time of  $8\mu s$ .

The short training symbols are generated by taking the IFFT of the following sequence for frequency bins  $-26$  to  $26$ :

$$S_{-26,26} = \sqrt{\frac{13}{6}} *$$

$$[0, 0, 1 + 1j, 0, 0, 0, -1 - 1j, 0, 0, 0, 1 + 1j, 0, 0, 0, -1 - 1j, 0, 0, 0, -1 - 1j, 0, 0, 0, 1 + 1j, 0, 0, 0, 0, 0, 0, -1 - 1j, 0, 0, 0, -1 - 1j, 0, 0, 0, 1 + 1j, 0, 0, ] \quad (6.30)$$

The last two frames of the preamble contain the long training symbols which are used for channel estimation and fine frequency acquisition.

The long training symbols are generated by taking the IFFT of the sequence

$$L_{-26,26} = [1, 1, -1, -1, 1, 1, -1, 1, -1, 1, 1, 1, 1, 1, 1, 1, -1, -1, 1, 1, -1, 1, -1, 1, -1, 1, -1, 1, -1, 1, -1, 1, -1, 1, 1, 1, 1, 0, 1, -1, -1, 1, 1, -1, 1, -1, 1, -1, -1, -1, -1, -1, 1, 1, -1, -1, 1, -1, 1, -1, 1, 1, 1, 1]. \quad (21)$$

The lack of copies in the OFDM frames is from the lack of zero packing in equation 21 and so the symbols have length  $Nfft$  and, along with the added cyclic prefix, the total length of the long training symbols is  $2.5 \times Nfft$ . Again, we set  $Nfft= 64$  so that the long training symbol is 64 samples

long. With a sample time of  $1/20MHZ = 0.05\mu s$  the long training symbol time is  $64 \times 0.05\mu s = 3.2\mu s$ . There are two long training symbols and a cyclic prefix of length 32 so the total time for the long training symbols is  $2 \times 3.2\mu s + 32 \times 0.05\mu s = 8\mu s$ .

#### 3.2.2 OFDM Frame Timing Estimation

Timing estimation is broken into two parts, frame timing or packet detection and symbol timing. In both cases we use the preamble for detection. Here we start with frame timing and exploit the periodicity of the short training symbols using the auto-correlation as described in [10]. From Appendix F, the cross-correlation function is defined as

$$f * g = \sum_{m=-\infty}^{\infty} \bar{f}[-m]g[m] \quad (22)$$

The correlation of the signal with a delayed copy of itself is defined as

$$A[n] = \sum_{k=0}^N r(k+n)\bar{r}[k+n+L] \quad (23)$$

where  $A[n]$  is the output,  $r[n]$  is the received sequence,  $L$  is the length of one short symbol and the length of the delay. There are several algorithms for coarse timing but all use the correlation properties of the short training symbols. In this analysis, the delay and correlate algorithm presented in [8] and [9] is used. Figure 6.24 shows the block diagram for this algorithm.

The top path,  $P(d)$ , contains the cross-correlator and the bottom path,  $R(d)$ , contains the auto-correlator. The  $\delta$  value in the bottom path is to avoid division by zero. The auto-correlator computes the power in the samples and is used to normalize the decision at the threshold detector. The cross-correlator takes advantage of the periodicity in the short training

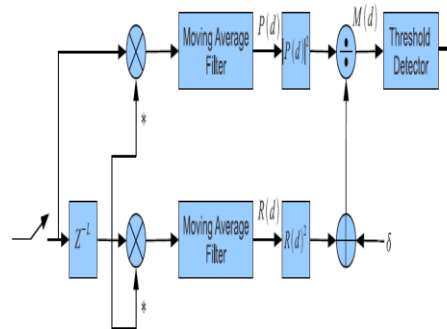


Figure 3 Delay and correlate algorithm.

symbols to locate the frame boundaries. These are defined mathematically as

$$P(d) = \sum_{m=0}^{L-1} r(d+m)\overline{r(d+m+L)} \quad (24)$$

$$R(d) = \sum_{m=0}^{L-1} |r(d+m+L)|^2 \quad (25)$$

where  $L$  is the length of the register in the moving average and  $r(d)$  is the  $d^{th}$  sample of the received signal.  $M(d)$  is the output of the correlator normalized by the received power and then tested against a threshold level. Squaring helps

mitigate the effects of large peak to average power ratios common in OFDM. The signal starts after the first 50 samples and because a length of 16 was used for the moving average filter, the maximum value of the correlation and the power is not reached for 16 samples. Also note that the timing estimate  $M(d)$  reaches a maximum at the 51st sample, which is the correct timing.

One might wonder why the auto-correlation is used in determining the frame start since the cross-correlation shows the symbol boundaries. The received signal will have a carrier frequency offset as well as multipath interference and Gaussian noise. For this reason the auto-correlation function is used to normalize the input to the threshold detector. Even with poor channel conditions the frame is still detected, although with a sample error. This sample error will need to be corrected with fine timing, or symbol timing estimation.

### 3.2.3 Frequency Offset Estimation

Estimation of frequency offset during the acquisition phase is performed in two parts. Coarse frequency offset uses the short training symbols and fine frequency offset uses the long training symbols. Both coarse and fine frequency estimation use the same algorithm, correlation with the received signal and a delayed copy. The conjugate product is then passed to a phase detector that outputs the phase error.

The maximum frequency offset between transmitter and receiver (for carrier frequency 5.825GHz) is

$$f\Delta = (40 \times 10^{-6})(5.825 \times 10^9) \quad (26)$$

$$= 233 \text{ KHz} \quad (27)$$

Hence any algorithm used to estimate and correct frequency offset needs to operate with this amount of offset. Suppose the received signal is

$$y(t) = x(t)e^{j2\pi f\Delta t} \quad (28)$$

where  $x(t)$  is the transmitted signal and  $f$  is the frequency offset. As stated previously, the short training symbols have a length of 16 samples or  $0.8\mu\text{s}$ . Then the output of the conjugate product from the correlation of the signal and the delayed copy is

$$y(t)y^*(t - \delta t) = |x(t)|^2 e^{j2\pi f\Delta(\delta t)} \quad (29)$$

The frequency offset is found by taking the arctangent of both sides

$$\Delta f = \frac{\angle y(t)y^*(t - \delta t)}{2\pi f\delta t} \quad (30)$$

where  $\delta t$  is the symbol time. The output of the phase detector is based on the arctangent function and thus has a range of  $[-\pi, \pi)$ . This means that the maximum detectable frequency offset using the conjugate product is

$$\Delta f = 625 \text{ KHz} \quad (31)$$

or about 107ppm at 5.825GHz, much greater than the allowable frequency offset. By comparison, using the long training symbols, the detectable frequency offset is

$$\Delta f = 156 \text{ KHz} \quad (32)$$

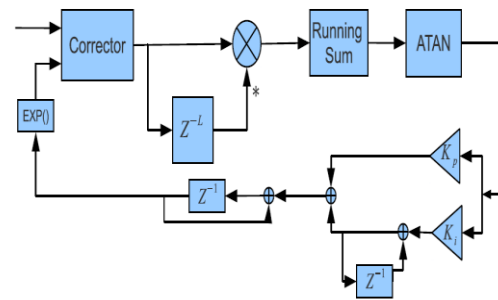


Figure 4 Frequency estimation algorithm.

This is why the short training symbols are used for the coarse estimation and correction before using the long training symbols for fine frequency estimation and correction.

Consider the example where the frequency offset is 200kHz. The poor phase estimation in the long training symbol portion is because the algorithm uses a delay length of 16 where the long training symbols have a length of 64. The previous example did not incorporate a phase locked loop (PLL) but instead the phase estimation of the entire preamble was computed and the average of the phase error was applied to the entire series. This is an impractical implementation because of the delay in waiting for the entire preamble to arrive. We now consider an example which uses a PLL with the same 200kHz frequency offset. By trial and error the values  $\theta_n = 2\pi/49$  and  $\zeta = \sqrt{2}/2$  were found making  $k_i = 0.0594$  and  $k_p = 0.1638$ . The accumulated phase of the variable controlled oscillator (VCO) and the VCO output. Notice that the frequency is correctly estimated but there is a phase offset in the VCO output. This is referred to as residual frequency offset and is dealt with using the pilot symbols.

Lastly, the constellation of the received signal with and without frequency offset compensation. The phase offset seen in the VCO output is also seen in the corrected constellation.

### 3.2.4 Symbol Timing Estimation

Symbol timing or fine timing is performed after coarse timing and after frequency offset correction. Fine timing estimation uses the cross-correlation of the known long training symbol with the received long training symbol to determine the start and end of an OFDM symbol and consequently the start and end of the FFT window. The cross correlation is sensitive to frequency offset and this explains the importance of correcting frequency offset before performing symbol timing estimation [6].

During the frame timing estimation, the starting edge of the packet was determined but within the packet symbol timing errors can be present. The cross-correlation of the known long training symbol and the received long training symbol can be determined by

$$r(n) = \sum_{m=0}^M r'_{LTS}(m)r_{LTS}(m-n)$$

where  $r'_{LTS}$  is the received long training symbols,  $r_{LTS}$  is the known long training symbol, and  $M$  is the length of the long training symbol. In Appendix F, it is shown that there



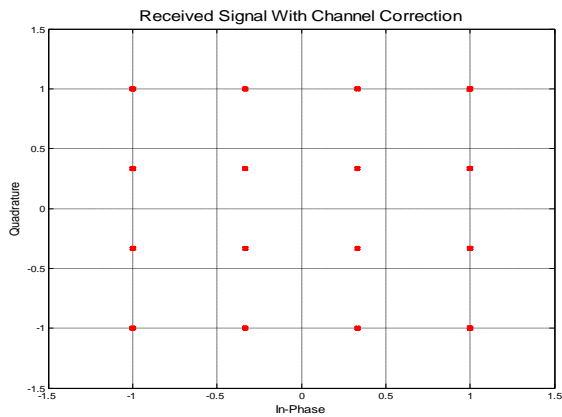


**Fig 8 Received constellation after channel correction**

From the fig 6 only frequency and timing offsets (synchronous errors) have been estimated and corrected. The effect of a multipath channel on the received constellation diagram is show in fig 6

To counter these effects, an equalizer is used. In a conventional single carrier system Equalization takes place in the time domain where the equalizer can be computationally Intensive. In an OFDM system, the equalization takes place in the frequency domain with the advantage that if the sub-channels are sufficiently narrow bands, the frequency fading of the channel can be considered flat within each sub-channel

It is common to average the equalizer gains over the two long training symbols to help mitigate the effects of the noise. Figure 7 shows the channel frequency response and the channel estimation using the above method. Notice that the noise in the channel affects the estimation. Figure 8 shows the received constellation after the channel estimation has been applied to Figure 6.

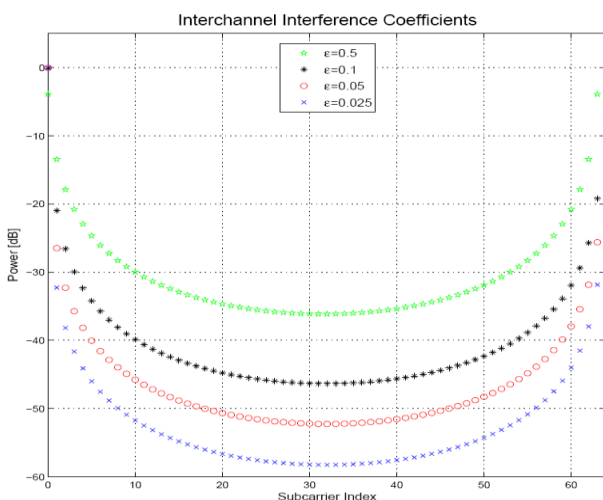


**Fig 9 ICI coefficients for  $\epsilon = 0.5, 0.1, 0.05, 0.025$ .**

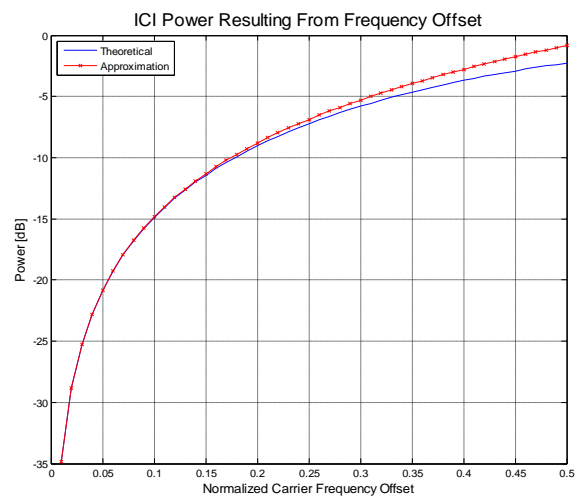


**Fig 10: Power of ICI.**

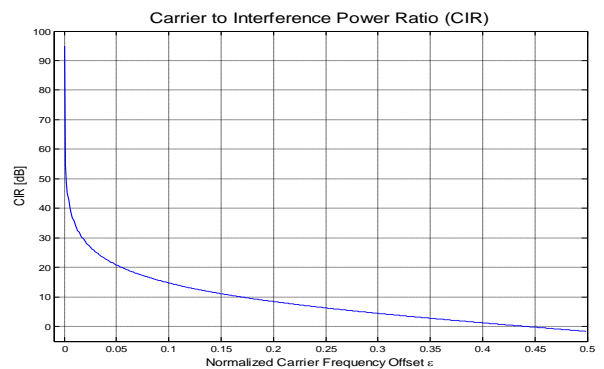


**Fig 11: Carrier-to-interference power ratio**

Notice that the frequency is correctly estimated but there is a phase offset in the VCO output. This is referred to as residual frequency offset and is dealt with using the pilot symbols. Lastly, the constellation of the received signal with and without synchronous error compensation and the phase error seen in the VCO output is also seen in the corrected constellation.

## 5. CONCLUSIONS

This paper proposes an improved preamble structure to achieve better timing synchronization in MIMO-OFDM, compared to the conventional Schmidl's and Minn's methods, the proposed preamble structures provide sharper correlation peak and could achieve improved Correct Detection Rate (CDR), thereby providing better timing synchronization. These improved algorithms not only eliminate the broad plateau problem but also mitigates the sub peaks.

### Future Scope:

The future work will involve the investigation and simulation of different probabilistic models in state of the art technologies such as 5G LTE

## REFERENCES

- [1] T.M. Schmidl, D. Cox, "Robust frequency and timing synchronization in OFDM," *IEEE Trans. on Comm.*, vol. 45, pp. 1613-1621, Dec. 1997.
- [2] H. Minn, M. Zeng, and V. K. Bhargava, "On timing offset estimation for OFDM systems," *IEEE Comm. Letters*, vol. 4, no. 7, pp. 242-244, July 2000.
- [3] Sicong Liu, Fang Yang, Jian Song, Fei Ren, and Jia Li, "OFDM Preamble Design for Synchronization Under Narrowband Interference" 2013 IEEE 17th International Symposium on Power Line Communications and Its Applications.
- [4] Leila Nasraoui, Leila Najjar Atallah, Mohamed Siala, "An Efficient Reduced-Complexity Two-Stage Differential Sliding Correlation Approach for OFDM Synchronization in the Multipath Channel", *IEEE Wireless Communications and Networking Conference*, 2012
- [5] Eric M. Silva C., Fredric J. Harris, G. Jovanovic Dolecek, "Synchronization Algorithms based on Weighted CAZAC Preambles for OFDM Systems", *International Symposium on Communications and Information Technologies (ISCIT)*, 2013
- [6] K. Murali, Dr.S.Sri Gowri and N.S.Murthy "A Novel Construction Technique for Design of Generalized Orthogonal Codes to Wireless Communication" *IJEE* (ISSN No. 0973-7383), Vol.- 1, Issue-2 of December 2009
- [7] B. P. Crow, I. Widjaja, L. G. Kim, and P. T. Sakai, "IEEE 802.11 wireless local area networks," *IEEE Commun. Mag.*, vol. 35, no. 9, pp. 116-126, Sept. 1997.
- [8] K.Murali., M.Sucharitha etc al.. "A Novel design of Time Varying Analysis of Channel estimation Methods of OFDM" on *International Journal of Management, IT & Engineering* (ISSN: 2249-0558) June 2012 Volume 2, Issue 6 (ICV 9.00)
- [9] C. Eklund, R. B. Marks, K. L. Stanwood, and S. Wang, "IEEE standard 802.16: a technical overview of the wirelessMAN air interface for broadband wireless access," *IEEE Commun. Mag.*, vol. 40, no. 6, pp. 98-107, Jun. 2002.
- [10] R. Frank, S. Zadoff, and R. Heimiller, "Phase shift pulse codes with good periodic correlation properties (corresp.)," *Information Theory, IRE Transactions on*, vol. 8, no. 6, pp. 381-382, October 1962.
- [11] Marey, M.; Steendam, H., "Analysis of the Narrowband Interference Effect on OFDM Timing Synchronization," *Signal Processing, IEEE Transactions on*, vol. 55, no. 9, pp. 4558-4566, Sept. 2007
- [12] K.Murali, N.Ramesh babu etc al., "Performance Analysis of CP-OFDM with Different fading channels with Energy Efficient Binary Power Control" on *(ISTP-JREEE)* in (Volume 3, Issue 4 July 14)